The Structure of Liquid Formamide Studied by Means of X-Ray Diffraction and *ab Initio* LCGO-MO-SCF Calculations

Hitoshi Ohtaki,* Atsushi Funaki, Bernd M. Rode,† and Gilbert J. Reibnegger†

Department of Electronic Chemistry, Tokyo Institute of Technology at Nagatsuta, Nagatsuta-cho, Midori-ku, Yokohama 227

†*Institute of Inorganic and Analytical Chemistry, The University of Innsbruck, Innrain 52a, Innsbruck A-6020, Austria*

(Received February 7, 1983)

The molecular and liquid structures of formamide have been studied by means of X-ray diffraction. Relative stabilities of aggregates of formamide molecules have been calculated by using the *ab initio* LCGO-MO-SCF procedure and minimal basis sets. The atomic distances within a formamide molecule and the intermolecular N···O distance between the hydrogen-bonded molecules are determined by the X-ray diffraction experiment as follows: C=O: 1.24(1) Å, C-N: 1.33(1) Å, N···O (intramolecular): 2.25(2) Å, and N···O (intermolecular): 3.05(5) Å. The intermolecular -HNH···O=C< bond angle (θ) is about 120°. It is concluded from the X-ray diffraction experiment that liquid formamide mainly consists of the chain-like hydrogen-bonded structure of formamide molecules by combining through $-NH_2\cdots O=CH-$ interactions. The conclusion is supported by the *ab initio* calculations. Formation of ring-dimers in the liquid formamide has not been confirmed by the X-ray diffraction study, although a possibility of the formation of the ring-dimer structure as another constituent of liquid formamide is suggested from the *ab initio* calculations.

Formamide ($HCONH_2$) has a relatively large dielectric constant ($\varepsilon/\varepsilon_0=107$ at 25 °C, where ε and ε_0 represent the dielectric constants of formamide and vacuum, respectively), and thus can dissolve many electrolytes. Since the oxygen and nitrogen atoms within a formamide molecule are negatively charged and the carbon and hydrogen atoms have partially positive charges, a formamide molecule has a dipole moment of about 12.4×10^{-30} C m *in vacuo*. The donor number of formamide ($DN=24$) is larger than that of water ($DN=18.0$), although the acceptor number of the former ($AN=39.8$) is smaller than that of the latter ($AN=54.8$). Therefore, rather strong interactions between formamide molecules can be expected in the condensed phase.

Molecular and crystal structures of formamide have been determined by X-ray and electron diffraction methods,[1,2] and it has been found that all atoms within one molecule lay on a plane. A similar structure is kept even in the gas phase.[3] Therefore, we can expect that molecules of formamide in the liquid state have the planar structure similar to that observed in the gas and solid phases.[1-3] In crystal, formamide molecules form ring dimers which construct a large ring structure through hydrogen bonds (see Fig. 1).[1,2] However, the stable ring structure exisiting in the solid state may be rather unfavorable to give the high dielectric constant of formamide and high solubilities of electrolytes in it in the liquid phase.

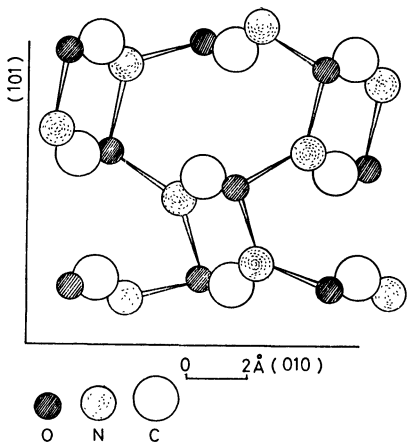

Fig. 1. Structure of formamide in the solid state,[1]

The aim of the present study is to determine the molecular arrangement, as well as the molecular structure of formamide in the liquid phase, in order to compare the structures with those in the gas and solid phases. The liquid structure of formamide estimated by the X-ray diffraction method will be compared with structural models of various aggregates examined by the *ab initio* LCGO-MO-SCF calculations.

Experimental

Preparation of Sample Solution. Formamide of reagent grade, purchased from Wako Pure Chemicals Co., Tokyo, was distilled twice under a reduced pressure. The water content of the formamide was determined by means of the Karl-Fischer titration. Since the amount of water (about 0.02% w/w) was very small, it was neglected in the course of the data analysis of X-ray diffraction.

Method of Measurement and Treatment of X-Ray Scattering Data. The X-ray diffractometer, JEOL DX-GO-Y (θ-θ type), was employed in combination with Philips 2255/20 Mo $K\alpha$ X-ray tube ($\lambda=0.7107$ Å) and an NaI-Tl scintillation counter. Scattered X-rays were monochromatized by a Johansson-type LiF monochromator and a pulse-height analyzer. The scattering angle (2θ) measured was in the range of 2° to 140°, and the data were recorded twice over the whole angle range. Corrections and analysis of the scattering data were performed by the same ways as those described elsewhere.[4] The scattering and correction factors of atoms in the system were taken from the literature.[5]

The reduced intensities $i(s)$ were obtained by the following equation:

$$i(s) = KI_{\mathrm{corr}}(s) - \sum_i n_i[\{f_i(s)+\Delta f_i'\}^2+(\Delta f_i'')^2], \qquad (1)$$

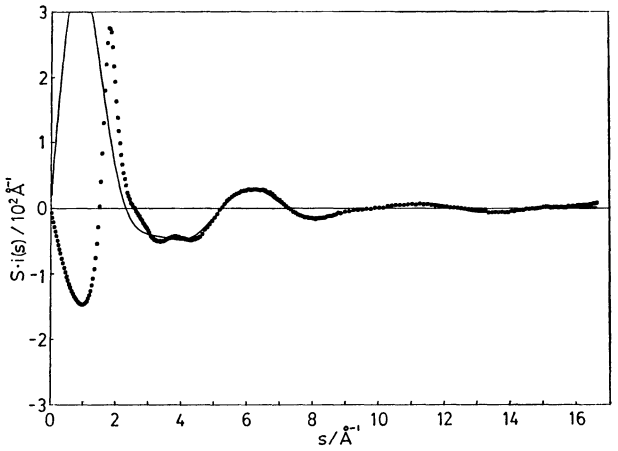

Fig. 2. Reduced intensities, $s \cdot i(s)$, experimentally obtained (circles) and calculated values ($s \cdot i_{\text{calcd}}^{\text{intra}}(s)$, solid line) by taking into account only intramolecular interactions.

where K denotes a factor for transforming measured intensities $I_{\text{corr}}(s)$, which had been corrected for absorption, polarization and multiple scatterings of X-rays by the usual methods,[4] to the absolute ones. The factor had been obtained by the high-angle method[6] and the method by Krogh-Moe[7] and Norman.[8] The K values obtained by the two methods agreed with each other within 1%. $\Delta f_i'$ and $\Delta f_i''$ in Eq. 1 represent the real and imaginary parts of the anomalous dispersion of atom i, respectively.

The reduced intensities multiplied by s ($=4\pi\lambda^{-1}\sin\theta$) of the test solution are shown in Fig. 2.

The radial distribution function $D(r)$ was calculated by the Fourier transform of the reduced intensities according to Eq. 2.

$$D(r) = 4\pi r^2\rho_0 + \frac{2r}{\pi}\int_0^{s_{\max}} s \cdot i(s) \cdot M(s) \cdot \sin(sr)\mathrm{d}s, \qquad (2)$$

where ρ_0 is the average scattering density in the stoichiometric volume V of the test solution, and $s_{\max}$ denotes the maximum s-value attained in the measurement ($s_{\max}=16.6$ Å^{-1}). $M(s)$ represents the modification function

$$M(s) = \frac{[\sum_i n_i f_i(0)^2]}{[\sum_i n_i f_i(s)^2]} \cdot \exp(-ks^2), \qquad (3)$$

where n_i denotes the number of atom i in the stoichiometric volume. $f_i(0)$ and $f_i(s)$ stand for the scattering factors of atom i at $s=0$ and s, respectively. The damping factor k was chosen as 0.01 Å^2 in the present experiment.

Calculations for data treatments were carried out by using the KURVLR program developed by Johansson and Sandström.[9]

Raman spectra of the test solution were measured before and after X-ray radiation, and it was confirmed that formamide was not decomposed by the X-ray radiation.

Computations for treating the X-ray data were performed at the Tokyo Intitute of Technology at Nagatsuta by using HITAC M-170.

Theoretical Treatment

In order to investigate the relative stabilities of various possible aggregates of formamide molecules in the condensed phase, varying structural models were examined by means of *ab initio* LCGO-MO-SCF calculations with a minimal basis set (2s/1p),[10] which has been successfully employed in other cases.[11-13] The molecular geometry of formamide was kept constant at the experimental values obtained by the present work, except for the C–H and N–H bond lengths which were taken from the literature,[2] throughout the calculations. The dimer models which were investigated by the *ab initio* calculations were selected on the basis of knowledges obtained by the present X-ray diffraction experiment. Some possible structural models were also examined in order to compare their relative stabilities with those of the selected geometries. The computations were carried out by using computers at the University of Innsbruck and partly at the Interuniversity Computer Center of the Technical University of Vienna.

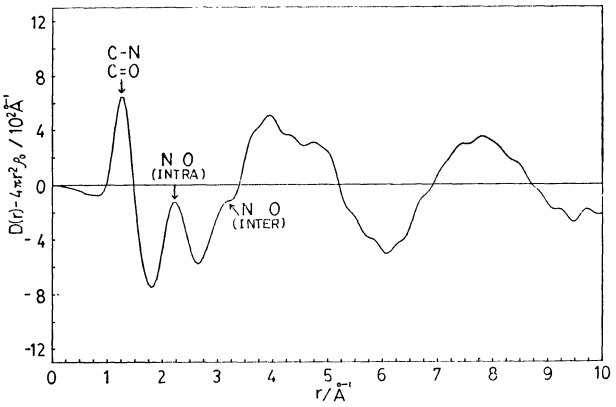

Fig. 3. Differential radial distribution curve of liquid formamide.

Results and Discussion

X-Ray Diffraction. The differential radial distribution curve, $D(r)-4\pi r^2\rho_0$, of formamide is shown in Fig. 3. The first peak appearing at about 1.2 Å is ascribed to the C–N and C=O bonds within a formamide molecule, and the second peak at 2.3 Å is attributed to the intramolecular N···O distance. A shoulder is observed at about 3 Å, which may be due to the intermolecular N···O distance according to the data by X-ray crystallography of formamide.[1,2] The reduced intensity curve calculated by using the intramolecular bond distances found from the differential radial distribution curve well reproduced the experimental curve in the range $s>5$ Å^{-1} (see Fig. 2). At the lower s range the two curves are remarkably discrepant, the discrepancy being due to intermolecular interactions between formamide molecules which have not been taken into account at the present stage of the X-ray data analysis.

The intramolecular distances thus roughly estimated from the differential radial distribution curve were further refined by applying the least-squares method to the reduced intensities $s \cdot i(s)$ over various s ranges, where $s_{\max}$ was fixed at 16.6 Å^{-1} and $s_{\min}$ was varied from 4 Å^{-1} to 6 Å^{-1}. The least-squares refinement was carried out by using the following equation:

$$U = \sum_{s_{min}}^{s_{max}} s^2\{i(s) - i_{calcd}^{intra}(s)\}^2, \quad (4)$$

where $i_{calcd}^{intra}(s)$ denotes the calculated $i(s)$ values by taking into account the intramolecular interactions only.

The results obtained for the intramolecular distances within a formamide molecules, as well as the temperature factors of each atom pair, in the liquid state are summarized and compared with those found in the gas and solid states in Table 1. No significant difference was noticed in the bond distances within a formamide molecule in the different phases.

At the second stage of the analysis of the X-ray scattering data, intermolecular interactions between formamide molecules in the liquid state were estimated from intensities due to the intermolecular interactions only which were obtained by subtracting the intensities due to the intramolecular interactions thus evaluated from the experimental values:

$$i^{inter}(s) = i(s) - i_{calcd}^{intra}(s). \quad (5)$$

Intensities $s \cdot i^{inter}(s)$ due to the intermolecular interactions thus estimated are shown in Fig. 4.

In order to interprete the $s \cdot i^{inter}(s)$ data, various dimer models were examined. In Fig. 5 the models examined are summarized. In each model the C–N and N–H bonds were rotated in order to compare the theoretical scattering intensities calculated from the models having various configurations with the experimentally obtained $s \cdot i(s)$ values. However, those except two models did not give theoretical intensities which satisfactorily fitted the experimental curves. The two models were the extremes of model (3) in Fig. 5. One was a linear dimer bonded through the N–H···O hydrogen bond with $\Theta=0°$ (two molecules were in the same plane) and $\Theta'=0°$ (Fig. 6A) and the other was a ring dimer ($\Theta=0°$ and $\Theta'=180°$) (Fig. 6B). A model at an intermediate configuration ($\Theta=0°$ and $0°<\Theta'<180°$) gave a theoretical intensity curve between those of the two extremes. In the course of the calculations of the theoretical intensity curve $s \cdot i_{calcd}^{inter}(s)$, the N···O distance was fixed at 3.05 Å in each model, which was experimentally determined by the present X-ray diffraction work. Theoretical intensities calculated on the basis of the two models were compared with the experimental ones in Fig. 4. The theoretical $s \cdot i_{calcd}^{inter}(s)$ curve drawn by using

TABLE 1. INTRA- AND INTERMOLECULAR DISTANCES OF FORMAMIDE. r AND b DENOTE THE BOND DISTANCE AND TEMPERATURE FACTOR, RESPECTIVELY[a)]

Bond	Liquid	Solid	Gas
C=O	$r=1.24(1)$ Å, $b=0.0017(3)$ Å^2	$r=1.24$ Å[2)]	$r=1.21$ Å[3)]
C–N	$r=1.33(1)$ Å, $b=0.0018(3)$ Å^2	$r=1.32$ Å[2)]	$r=1.37$ Å[3)]
N···O (intra)	$r=2.25(2)$ Å, $b=0.0028(5)$ Å^2	$r=2.27$ Å[2)]	$r=2.29$ Å[3)]
N···O (inter)	$r=3.05(5)$ Å	$r=2.88$ Å[1)], 2.94 Å[1)]	

a) Numbers in parentheses indicate standard uncertainties.

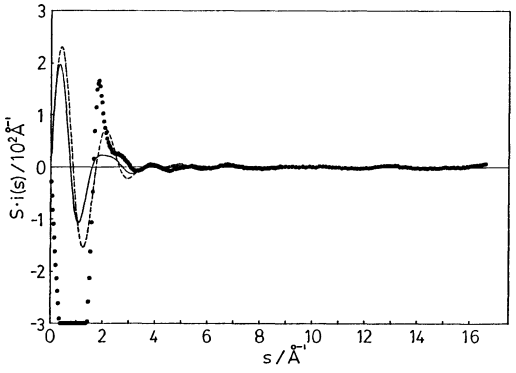

Fig. 4. Reduced intensities, $s \cdot i^{inter}(s)$, defined by Eq. 5 (circles). The solid and broken lines represent calculated $s \cdot i(s)$ values for intermolecular atom-pair interactions in models (A) and (B) given in Fig. 6, respectively.

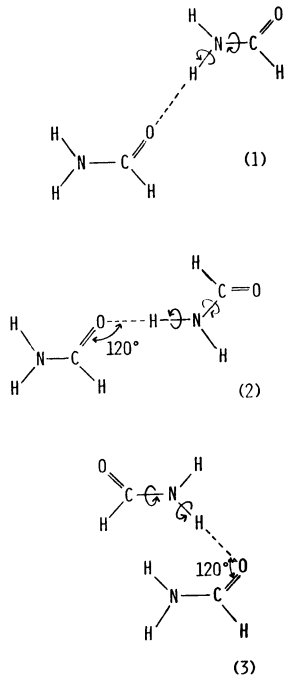

Fig. 5. Structural models of various dimers. The second molecule is allowed to rotate along the C-N and O···H-N bonds.

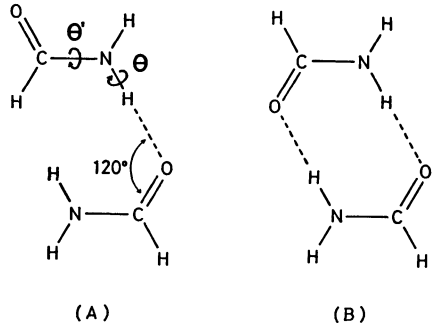

Fig. 6. Structural models of linear (A) and cyclic (B) dimers of formamide.

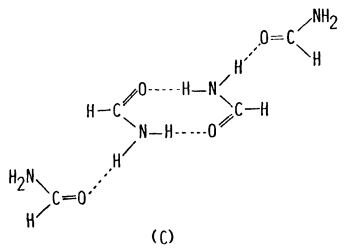

(C)

Fig. 7. A structural model consisting of linear and cyclic constituents.

the linear dimer model shown in Fig. 6A gave a better agreement with the experimental values than that calculated from the ring dimer model (Fig. 6B) in the range 3.5 Å^{-1}<s<5.5 Å^{-1}, and moreover, the hump appearing around $s\simeq 2.8$ Å^{-1} was better reproduced by the former model than the latter.

A possibility of formation of a mixture of the two models were also examined at various mole ratios. However, an increase in the content of the ring dimers in the mixture enhanced the discrepancy between the theoretical and experimental intensity curves in the range 2.5 Å^{-1}<s<3.5 Å^{-1}, and therefore, the mixture model could not give a satisfactory interpretation for the $s\cdot i^{\text{inter}}(s)$ curve.

A chain-like structure consisting of the linear and the ring dimer units was taken into consideration in order to interprete the experimental $s\cdot i^{\text{inter}}(s)$ curve. The model employed is shown in Fig. 7 (model C). However, no noticeable improvement could be achieved in the interpretation of the experimentally obtained $s\cdot i^{\text{inter}}(s)$ curve by the introduction of the mixture model.

The intra- and intermolecular distances thus determined on the basis of the linear dimer model are summarized in Table 1. Disagreement between the experimental and theoretical $s\cdot i(s)$ curves observed at s<3.5 Å^{-1} is due to a disregard of longer range intermolecular and inter-chain interactions.

Although the linear model gave a better interpretation than the ring model for the experimental X-ray scattering data, the difference between the $s\cdot i(s)$ curve calculated by using the two models was so small that the existence of the ring dimers in the liquid formamide could not be completely excluded by the X-ray diffraction method examined in the present study. Therefore, we examined *ab initio* calculations for estimating energies of intermolecular interactions between formamide molecules in order to compare relative stabilities of the linear and ring dimer structures.

Ab Initio *LCGO-MO-SCF Calculations.* Relative stabilities of intermolecular interactions of dimeric, trimeric and even tetrameric polymers of formamide were calculated by the *ab initio* LCGO-MO-SCF procedure with a minimal basis set, which had been employed for calculations in other systems.[10–13] The geometry of the formamide molecules was kept constant at the experimental values given in Table 1 which were obtained by the present work, except for the C–H and N–H distances which were taken from the literature,[1] throughout the calculations, and the intermolecular –NH_2···O=CH– distances were allowed to change in order to search the energy minimum of the interaction at a given aggregate model.

Table 2. Energies at optimized C-H···O and N-H···O hydrogen bond distances (R) and energies per hydrogen bond (E_h) within formamide dimers[a]

Model	R/Å	E_h/kJ mol^{-1}
(a) 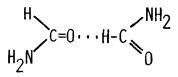	3.27	−8.4
(b) 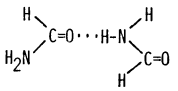	2.75	−43.9
(c) 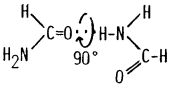	2.80	−45.2
(d) 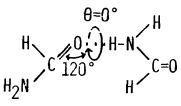	2.80	−67.8
(e) 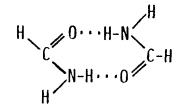	2.80	−63.2

a) The total energy of monomer is −143.34210 hartrees. 1 hartree=2625.34 kJ mol^{-1}.

For dimers, five different models as shown in the first column of Table 2 were examined as selected ones on the basis of considerations described in the previous section for the X-ray diffraction experiment. In models (a), (b), (d), and (e) we assumed that the two molecules were situated in the same plane. In model (c), on the other hand, the planes containing each molecule differed by 90°.

The optimized distance (R) of the intermolecular hydrogen bonds and energies for each hydrogen bonding (E_h) are listed in Table 2. In agreement with previous results,[14,15] model (d) gave the largest stabilization energy for the hydrogen bonding among the chain-like structures examined here. The stabilization energy for the formation of the dimers becomes largest in model (e), because the dimer has two hydrogen bonds within the unit structure (*i.e.*, −63.2 kJ per hydrogen bond×2=−126.4 kJ per dimer). Thus we can say that the cyclic structure is most stable in the formation of dimeric formamide. Nevertheless, as we will discuss in later sections, the structure shown in the linear model (d) can be more favorable than the cyclic dimer model (e) at a high degree of polymerization of the molecules in the condensed phase in which a large number of formamide molecules interact each other.

In model (d) the change in the relative stability of the linear dimer with changing angle of rotation (Θ in Fig. 6A) of the second molecule around the axis of the hydrogen bond was examined. The changes in the total energy (ΔE_{tot}) by the rotation are tabulated in Table 3. A shallow minimum appeared at

Table 3. The energy change (ΔE_{tot}) of the linear dimer model (d) at various rotation angles (Θ)

Θ/°	ΔE_{tot}/kJ mol^{-1}
0	—
30	6.7
60	9.7
90	7.5
120	9.5
150	11.6
180	11.6

Θ=90°, which suggested that the rotated structure of model (d) could have some contribution to the liquid structure of formamide, although the minimum was very shallow and the basis set employed in the present calculations was not highly sophisticated.

The hydrogen-bond distance between two formamide molecules through either C–H···O or N–H···O interaction was calculated by optimizing the distance at the lowest energy of interactions of a given configuration of the formamide dimers by the *ab initio* method (Table 2). Except for model (a) which had a longer hydrogen bond than the experimental value (3.05 Å), the distance found in models (b) to (e) was in the range 2.75—2.80 Å independent of the configurations. The result suggested that the intermolecular hydrogen-bonded distance of formamide molecules is rather insensitive to the molecular arrangement.

The distances of the hydrogen bond in models (b) to (e) were all slightly shorter than the observed value. The shortening of the calculated distance of the hydrogen bond may mainly be due to a more or less simplified basis set used in the present calculations, although the minimal basis set employed in the present calculations can give rather reasonable distances for hydrogen bonds between molecules compared with other minimal basis sets used so far.[16]

Stabilization energies of formation of trimers were estimated by the same procedure for five kinds of trimeric aggregates, four of them being shown in Fig. 8. The other one is the trimeric moiety of the chain-like structure of the mixed linear-and-ring structure shown in Fig. 7 (structure C). The energy of the hydrogen bonds within the last trimer model was a simple sum of the energies of the linear dimer (d in Table 2) and the ring dimer (e), *i.e.* ($-67.8+(2\times -63.2)$) kJ per trimer. The stabilization energies of the other trimers shown in Fig. 8 are summarized in Table 4. Structure (II), which is an extension of the linear dimer (d) (or model A in Fig. 5), has the largest energy per hydrogen bond among the five models. However, the total energy of stabilization of the trimers is largest in the mixed linear-and-ring model. Therefore, this type of the chain-like structure may contribute to some extent to the construction of liquid formamide, although the existence of the ring-dimer structure was not well accepted as the model explainable for the X-ray diffraction data.

It should be noted that the energy of hydrogen bonding in the formation of trimer (II) was the same as that in dimer (d). This result suggests that the

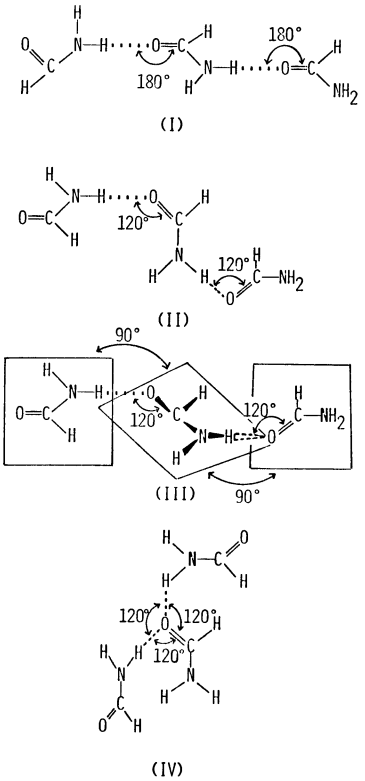

Fig. 8. Structural models of trimers.

Table 4. Stabilization energies for trimeric structures due to hydrogen bonding (E_h)

Model	E_h/kJ mol^{-1}
(I)	−48.5
(II)	−67.8
(III)	−60.2
(IV)	−44.4

energy of hydrogen-bonding of this type seems to be additive. On the other hand, trimer model (I), which is an extension of dimer (b), had an increased energy of the hydrogen bond by polymerization, although the stabilization energy of the formation of trimer (I) was still smaller than that of trimer (II). A relatively large stabilization energy of the hydrogen bond in trimer (III) suggested that rotation of molecules in trimer (II) might be easy. Trimer (IV) seems to be rather unstable compared with trimers (II) and (III) and has almost the same stability as trimer (I).

Stabilization energies for the formation of some tetramers were also calculated. For a tetramer similar to trimer (I) (*i.e.*, a linear polymer with the N–H···O angle of 180°), a slight increase by 1.3 kJ mol^{-1} (the total energy of the hydrogen bond was −49.8 kJ mol^{-1}) was observed in the stabilization energy of the aggregate, which was much less than the increment in the formation of trimer (I) from dimer (b) (4.6 kJ mol^{-1}). This suggests that the stabilization energy due to hydrogen bonding of this type may reach a constant value of about −50 kJ mol^{-1} at a pentamer or a hexamer of formamide. Since the stabilization energy of the formation of hydrogen bonds of this type is much

less compared with that of the type of dimer (d) or trimer (II) (67.8 kJ mol^{-1}), the chain-like structure of the trimer (I)-type may be less important in liquid formamide. The stabilization energy per hydrogen bond of the trimer (II)-type (or the dimer (d)-type) within a linear tetramer was essentially the same as that of the corresponding trimer and dimer, which indicated that the additivity of the stabilization of the aggregates was held in this configuration, and the chain structure of this type thus becomes the most stable one in liquid formamide.

Although the ring dimer has a larger stabilization energy due to the formation of two hydrogen bonds within it than any of the open-chain structures examined, the open structure consisting of dimer (d)-units becomes more stable than the ring structure, if the chains is formed with more than 16 molecules. Entropy effects due to easier bond rupture between molecules in the chain structure than in the ring structure and due to rotation of molecules in the chain will probably make the chain structure more favorable than the ring structure, so that the number of molecules for polymerization necessary to form stable chains might be much less than 16. Thus it can be concluded from the results of the MO-calculations that the open structures consisting of the trimer (II)-units and, to some extent the trimer (III)-units, should be dominant in liquid formamide. The ring-dimer structure may contribute to some extent to the chain structure as a link between the linear chain structures, as indicated in structure C, although the contribution was not detectable by the X-ray diffraction experiments.

A long chain structure and a mixed linear-and-ring structure did not give improved interpretations to the X-ray diffraction data, because interactions between the chain structures could hardly be estimated in the interpretation of the intensities of scattered X-rays.

The work has been partially supported by the Grant-in-Aid for Special Project Research (No. 510806) from the Ministry of Education, Science and Culture of Japan, and by the International Research Cooperation Project (Erl. zl. 18 889/25-10/79) from the Austrian Federal Ministry.

References

1) J. Ladell and B. Post, *Acta Crystallogr.*, **7**, 559 (1954).
2) E. D. Stevens, *Acta Crystallogr., Sect. B*, **34**, 544 (1978).
3) M. Kitano and K. Kuchitsu, *Bull. Chem. Soc. Jpn.*, **47**, 67 (1974).
4) H. Ohtaki, M. Maeda, and S. Ito, *Bull. Chem. Soc. Jpn.*, **47**, 2217 (1974); H. Ohtaki, T. Yamaguchi, and M. Maeda, *ibid.*, **49**, 701 (1976); T. Yamaguchi and H. Ohtaki, *ibid.*, **51**, 3227 (1978).
5) A. H. Compton and S. K. Allison, "X-Ray in Theory and Experiment," Van Nostrand, New York (1935); R. F. Stewart, E. R. Davidson, and W. T. Simpson, *J. Chem. Phys.*, **42**, 3175 (1964); D. T. Cromer and J. T. Waber, *Acta Crystallogr.*, **18**, 104 (1965); D. T. Cromer, *J. Chem. Phys.*, **50**, 4857 (1969); D. T. Cromer and D. Liberman, *ibid.*, **53**, 1891 (1970).
6) K. Furukawa, *Rep. Prog. Phys.*, **25**, 395 (1962).
7) J. Krogh-Moe, *Acta Crystallogr.*, **9**, 951 (1956).
8) N. Norman, *Acta Crystallogr.*, **10**, 370 (1957).
9) G. Johansson and M. Sandström, *Chem. Scr.*, **4**, 195 (1973).
10) B. M. Rode and K. Sagarik, *Chem. Phys. Lett.*, **88**, 337 (1982).
11) R. Fusseneger and B. M. Rode, *Chem. Phys. Lett.*, **44**, 95 (1976).
12) B. M. Rode and R. Fussenegger, *J. Chem. Soc., Faraday Trans. 2*, **71**, 1958 (1975).
13) J. F. Hinton and R. D. Harpool, *J. Am. Chem. Soc.*, **99**, 346 (1977).
14) A. Pullman, H. Berthod, C. Giessner-Prettre, J. F. Hinton, and D. Harpool, *J. Am. Chem. Soc.*, **100**, 3991 (1978).
15) N. R. Carlsen, L. Random, N. V. Riggs, and W. R. Rodwell, *J. Am. Chem. Soc.*, **101**, 2233 (1979).
16) Minimal basis sets such as the STO-3G basis set sometimes give a very short distance for a hydrogen-bond compared with hydrogen-bond distances calculated by extended basis sets. The basis set employed here has a much small effect for the shortening of the calculated distances of hydrogen-bonds. An example may be given for an O···N distance in an NH_3-H_2O system, in which the O···N distance has been estimated to be 3.000 Å by using the present (2s/1p) basis set (B. M. Rode and K. Sagarik, *Chem. Phys. Lett.* **88**, 337 (1982)) and 3.075 Å by a more extended basis set (8s/4p/1d).